Acta Metall. Sin. (Engl. Lett.), 2014, **27**(3), 469–475
DOI 10.1007/s40195-014-0066-y

Effect of Heat Treatment on Microstructures and Mechanical Properties of Hot-Dip Galvanized DP Steels

Enbao Pan · Hongshuang Di · Guangwei Jiang · Chengren Bao

Received: 10 April 2014 / Revised: 30 April 2014 / Published online: 12 June 2014

Abstract In order to simulate the hot-dipped galvanizing of dual-phase (DP) steel (wt%) 0.15C–0.1Si–1.7Mn, the DP steels were obtained by different annealing schedules. The effects of soaking temperature, time, and cooling rate on ferrite grain, volume fraction of martensite, and the fine structure of martensite were studied. Results showed that the yield strength (YS) of DP steel is sensitive to annealing schedule, while total elongation has no noticeable dependence on annealing schedule. Increasing soaking temperature from 790 to 850 °C, the YS is the lowest at soaking temperature of 850 °C. Changing CR1 from 6 to 24 °C/s, the YS is the highest when CR1 is 12 °C/s. Increasing soaking time from 30 to 100 s, the YS is the lowest at soaking time of 100 s. Besides, it was found that sufficient movable dislocations within ferrite grains and high martensite volume fraction can eliminate yield point elongation, decrease the YS, and increase ultimate tensile strength. Through TEM observations, it was also found that increasing annealing temperature promotes austenite transformation into twin martensite, and increases volume fraction of martensite at sufficient cooling rate. With increasing the martensite volume fraction, the deformation substructure in the ferrite is well developed.

KEY WORDS: Advanced high strength steels (AHSS); Dual-phase (DP) steel; Microstructure; Annealing temperature

1 Introduction

In recent years, advanced high strength steels (AHSS), including dual-phase (DP) steels, transformation-induced plasticity (TRIP) steels, twinning-induced plasticity (TWIP) steel, complex phase (CP) steels, and martensitic steels (MART), have been increasingly used in automotive bodies for lightweight and crash-safe designs [1–3]. In particular, as one kind of AHSS, DP steels are widely used in various vehicle components because of their favorable combination of strength, high work-hardening rate, elimination of yield point elongation, ductility, and formability over other high strength low alloy (HSLA) steels with similar yield strength (YS) [4–6]. These favorable behaviors of DP steels come from the combined properties of the hard martensite phase with high strength and the soft ferrite matrix with good ductility [7, 8].

Regarding the cold-rolled and annealed DP steel sheets, as typical steels, the ferrite–martensite microstructure is formed during annealing which is usually carried out in a hot-dip galvanizing line [9, 10]. In this process, the cold-rolled steel with a ferrite–pearlite microstructure is reheated to the intercritical region, i.e., $\gamma + \alpha$ two-phase region, leading to the formation of austenite and ferrite phases. The

Available online at http://link.springer.com/journal/40195

E. Pan · H. Di (✉) · G. Jiang
State Key Laboratory of Rolling and Automation, Northeastern University, Shenyang 110189, China
e-mail: dhshuang@mail.neu.edu.cn

G. Jiang
Benxi Iron and Steel Co., Ltd., Benxi 117021, China

C. Bao
Shougang Jingtang United Iron & Steel Co., Ltd., Tangshan 063200, China

metastable austenite phase can be transformed to martensite or some of the other low-temperature transformation products during subsequent cooling which includes also a short holding at the temperature of the zinc bath, i.e., at approximately 460 °C [11–13].

However, volume fraction, grain size, distribution, and morphology of martensite as well as ferrite may significantly depend on details of the processing routes and are expected to be different in intercritical annealing processes. Furthermore, volume fraction, grain size, and morphology of martensite with ferrite may affect the final mechanical properties of the steel sheets. Given the complexity of DP steels, and the dynamic processes of deformation and fracture, studying the microstructure effects on deformation and fracture is of compelling interest. The mechanical properties of DP steels depend on various factors such as martensite and ferrite micromechanical properties, volume fraction, and morphology of martensite, as well as ferrite grain size [8, 14, 15]. Different mechanical properties for ferrite and martensite phases in dual/multi-phase steel have been reported by various researchers [16, 17]. Many researches revealed that the martensite volume fraction as well as the martensite carbon content is a dominant factor controlling the mechanical properties of DP steels [6, 18, 19]. Fine grain size, high strength, and high volume fraction of the martensite phase generally increase the tensile strength of DP steels.

As expected, a high volume fraction of the martensite phase reduces the ductility of DP steels. Furthermore, several previous studies showed that other microstructural variables, such as grain size of ferrite, morphology, and distribution of martensite particles, are also important [20, 21]. In addition, retained austenite in dual-phase steel is also considered to improve the ductility and increase the strain-hardening rate due to its transformation to martensite during straining [22].

Although considerable researches have been conducted on microstructures and mechanical properties of DP steels, but more investigations are still needed to precisely predict these properties. Moreover, in order to obtain the less scattering of mechanical properties in hot-dip galvanized DP steels, precise microstructures control considering annealing process is quite important. Thus, it is worth further investigating the possibility of achieving high strength as well as sufficient ductility by optimizing the annealing process parameters.

In this context, the present study aims to obtain suitable microstructures and thus good mechanical properties of DP780 cold rolling strip in order to simulate the hot-dipped galvanizing through optimizing the annealing process parameters. The tensile properties of the experiment steel were examined, and the microstructures were also observed.

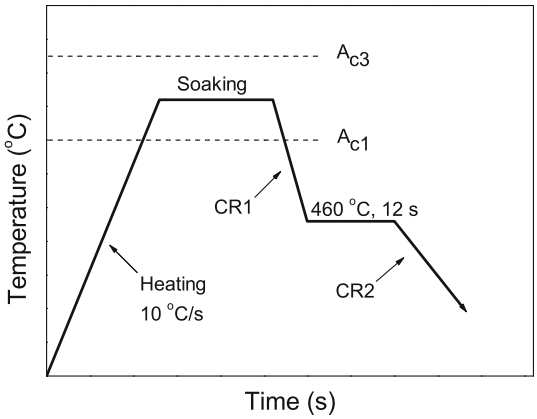

Fig. 1 Schematic diagram of annealing process

Table 1 Parameters for heat treatment schedules for different specimens

Specimen No.	Soaking temperature (°C)	Soaking time (s)	CR1 (°C/s)	CR2 (°C/s)
1	790	30	12	12
2	820	30	12	12
3	850	30	12	12
4	850	30	6	12
5	850	30	12	7
6	850	30	24	7
7	850	45	24	7
8	850	100	24	7

A relation of microstructures of this DP steel with the tensile properties was finally discussed.

2 Experimental

The chemical composition (in wt%) of the as-received cold rolling steel used in this work is 0.15C–0.1Si–0.04Al–0.09Ti–1.7Mn and Fe balanced. Specimens with dimension of 600 mm × 300 mm × 1.6 mm were cut from the cold-rolled strip along the longitudinal direction. In order to determine the annealing temperature range, thermal–mechanical simulation test was carried out on MMS-200 thermal mechanical simulator to measure temperature for the austenite formation. Dilatometer study indicated that the start temperature A_{c1} and the finish temperature A_{c3} of the pearlite-to-austenite transformation are 720 and 870 °C at the heating rate of 2 °C/s, respectively.

To obtain the dual-phase microstructures with varying the martensite morphologies, the specimens were subjected to different heat treatment schedules in order to simulate

Table 2 Mechanical properties and martensite volume fractions of different specimens

Specimen No.	YS (MPa)	UTS (MPa)	YS/TS	TEL (%)	MVF (%)
1	550	800	0.69	18.5	7.0
2	485	785	0.62	18.0	15.7
3	463	840	0.55	18.0	19.6
4	413	780	0.53	17.0	12.9
5	472	775	0.61	18.0	15.9
6	440	800	0.55	21.5	13.7
7	476	840	0.57	19.5	14.6
8	369	805	0.46	20.0	15.4

continuous annealing. Figure 1 shows the schematic diagram of annealing process.

The specimens were first reheated to intercritical "$\alpha + \gamma$" region, or to different temperatures, and held different times for soaking, respectively. Then, the specimens were cooled to 460 °C at a cooling rate of CR1 and held at this temperature for 12 s to simulate the hot-dipped galvanizing process. After that, the specimens were cooled to room temperature at a cooling rate of CR2. The continuous annealing simulation was carried out on the continuous anneal simulator developed by the State Key Laboratory of Rolling and Automation (RAL). During the experiment, nitrogen was used to protect the steel from oxidation and to cool the specimens. Table 1 lists the detailed parameters for heat treatment schedules.

Tensile specimens were cut from the annealed samples along the longitudinal direction and machined in accordance with GBT228-2002. Universal tensile testing machine (CCKX WAW-1000) was used to measure the tensile mechanical properties. The samples for microstructural observation were mechanically polished and etched with LePera's solution. The optical microscope (Leica Q550IW) was used to observe microstructures of the specimens.

Thin foils for transmission electron microscopy (TEM) observation were electropolished in Struer's Tenupol twin-jet polisher using a solution containing 93 vol% alcohol and 7 vol% perchloric acid. They were then observed in a TEM (FEI Tecnai G2 F20) at the operating voltage of 200 kV.

3 Results and Discussion

3.1 Mechanical Properties

The mechanical properties including YS, ultimate tensile strength (UTS), and total elongation (TEL) are given in Table 2, and the martensite volume fractions (MVF) are also shown in Table 2. The effect of annealing parameters, i.e., soaking temperature, cooling rate, and soaking time, on YS and UTS has been included in Fig. 2, where specimens Nos. 1–3 are for soaking temperature, specimens Nos. 4–6 are for cooling rate CR1, and specimens Nos. 6–8 are for soaking time. The representative stress–strain curves are shown in Fig. 3.

It is obvious in Fig. 2a that when the cooling rates CR1 and CR2 are both 12 °C/s, UTS of this DP steel increases and YS decreases with increasing the annealing temperature. In Fig. 2b, it can be seen that UTS of this DP steel has no obvious change, and YS was changed significantly when the soaking temperature is 850 °C, although cooling rates CR1 and CR2 were changed. Figure 2c displays the highest UTS and YS when the soaking temperature is 850 °C and soaking time is 45 s. In general, Fig. 2 shows the impact of annealing parameters on YS more significantly than UTS. The reason can be inferred that YS is mainly affected by ferrite grain size as well as dislocations in ferrite grain and UTS is mainly affected by martensite and ferrite.

Figure 3 shows the engineering stress–strain curves of the DP steel specimens Nos. 1–3. As it can be seen from Fig. 3, there is a yield point elongation when annealed at 790 and 820 °C. The specimen No. 1 has YS of 550 MPa and a tensile strength of 800 MPa after annealed at 790 °C. When the annealing temperature was increased to 820 °C, the yield and ultimate tensile strengths of specimen No .2 were decreased, and the yield point elongation was reduced. When the annealing temperature is increased to 850 °C, the YS was further decreased, but the UTS was significantly increased to 840 MPa.

The stress–strain curve of specimen No. 3 shown in Fig. 3 shows the typical characteristics of DP steels: low elastic limit, the absence of a distinct yield point, continuous yielding, and high initial strain-hardening rate. These features can be attributed to the enough mobile dislocations in ferrite nearby martensite created by transformation to martensite during cooling, and to residual stress [7]. The low elastic limit is thus suggested to be generated by the combined effects of the present elastic stresses that facilitate plastic flow and the additional dislocation, which is assumed to be partly mobile during early stages of yielding. Dislocation–dislocation interactions, dislocation pile-ups at ferrite/martensite interfaces, and the corresponding long-range elastic back stresses contribute to rapid strain hardening [23].

Compared with specimen No. 3, the specimens No. 1 and No. 2 have yield point elongation and high YS which are due to the absence of a substantial amount of martensite [22]. Speich [24] pointed out that at lower temperatures, the segregation of carbon to dislocations and the elimination of the residual stresses result in an increase in the YS and return of discontinuous yielding, but only under the

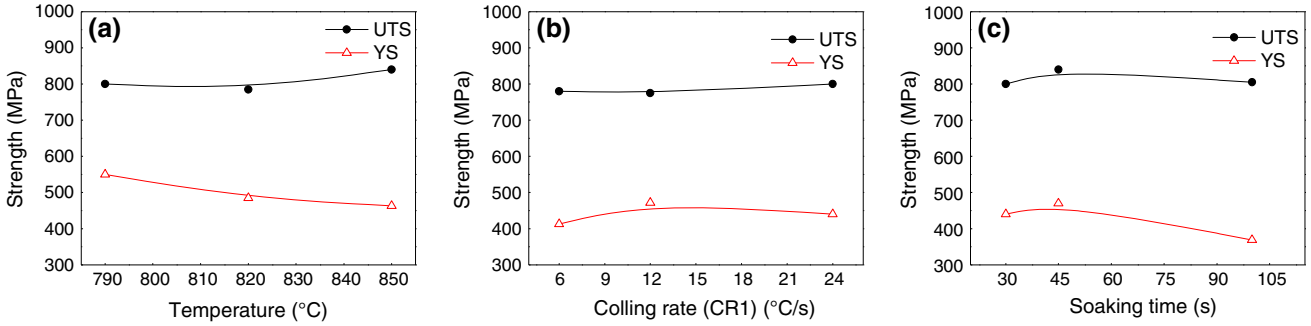

Fig. 2 Variation of annealing parameters on yield and ultimate tensile strengths of DP steel: **a** strength vs. soaking temperature for specimens Nos. 1–3; **b** strength vs. cooling rate CR1 for specimens Nos. 4–6; **c** strength vs. soaking time of specimens Nos. 6–8

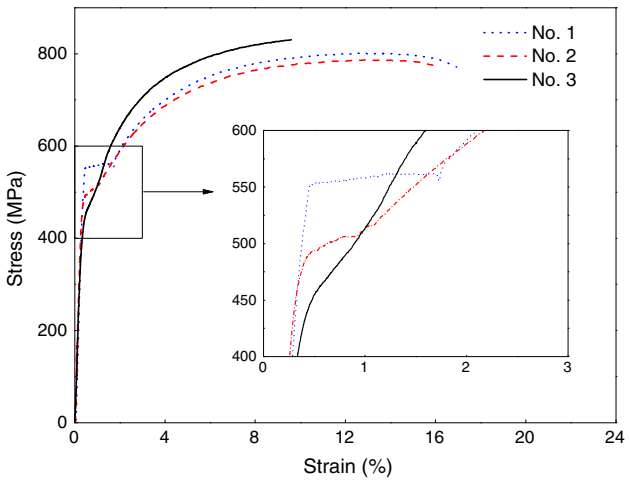

Fig. 3 Stress–strain curves of specimens Nos. 1–3

condition of the volume fraction of the martensite, phase is below 30%.

3.2 Microstructural Characterization

Figure 4 shows optical micrographs of the experimental steels after heat treatment. As shown in Fig. 4, the white is martensite or martensite–austenite island, and the gray phase is ferrite. From Fig. 4a–h, it is observed that there are relatively large ferrite grain size in Fig. 4d, h and there are relatively more MVF in Fig. 4c. When the annealing temperature is 790 °C (Fig. 4a), pearlite cannot fully transform to austenite. Thus, there are a large number of pearlite colonies, and only a small amount of island martensite is distributed among ferrite grains, as shown in Fig. 4a. Due to the low temperature and short holding time, austenite did not fully nucleate and grow up. After nucleation, austenite grows along the ferrite grains boundaries. During the cooling process, only a little austenite transforms into martensite along the ferrite grain boundaries and forms martensite in the ferrite grain boundaries.

When the annealing temperature is 820 °C (Fig. 4b), large amount of austenite nucleates. Therefore, much pearlite along the deformation band transforms into austenite. However, the austenite does not grow toward its neighboring ferrite grains. During the cooling process, most of the austenite transforms into martensite to form banded structure, as shown in Fig. 4b. The volume fraction of martensite annealed at 820 °C is higher than that at 790 °C.

When annealed at 850 °C (Fig. 4c), almost all the pearlite transform into austenite. At the same time, due to the sufficient nucleation and growth of austenite, some ferrite transforms into austenite. During the cooling, more austenite transforms into martensite and some austenite transforms into ferrite. The formation of the ferrite alleviates the banded microstructure. As a result, the volume fraction of the martensite annealed at 850 °C is the highest among the three annealing temperatures.

Figure 5 shows the TEM images corresponding to specimens Nos. 1–3. For specimens No. 1 and No. 2, most of the martensite or martensite–austenite is lath like. However, for specimen No. 3, most of the martensite is twinned. This results from the fact that when annealing temperature is low, only a little austenite is formed. While annealing temperature is high, a large amount of austenite is produced. So, super-cooled austenite is stable and transforms into twin martensite in cooling process. With increasing the heating temperature, microstructure becomes complex, as shown in Fig. 5c. Besides there is island martensite, there are also twin martensite and retained austenite. When heating temperature increases, pearlite transforms into austenite. At the same time, ferrite by side pearlite transforms into austenite. So the carbon content of austenitic region is distributed unevenly, and austenite stability is different [25, 26]. As a consequence, in the process of cooling, the microstructure becomes complex. First, edge austenite transforms into ferrite. Low carbon content austenite transforms into lath martensite. High carbon content austenite transforms into twin

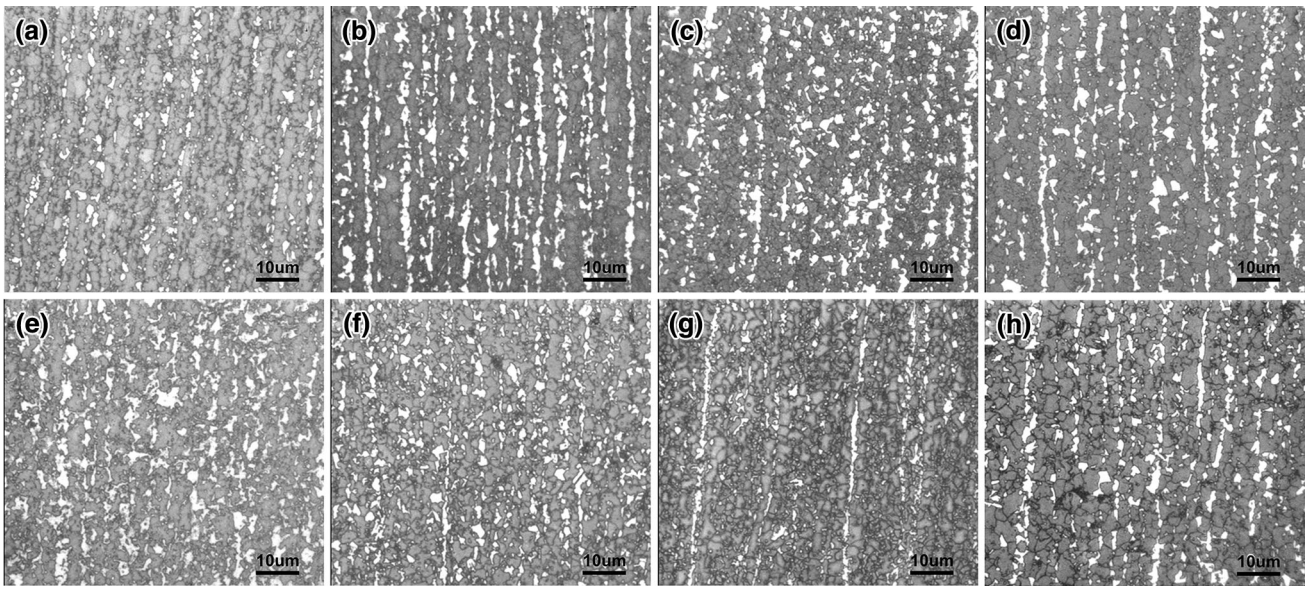

Fig. 4 Optical micrographs of the DP steel processed under different conditions: **a** specimen No. 1; **b** specimen No. 2; **c** specimen No. 3; **d** specimen No. 4; **e** specimen No. 5; **f** specimen No. 6; **g** specimen No. 7; **h** specimen No. 8

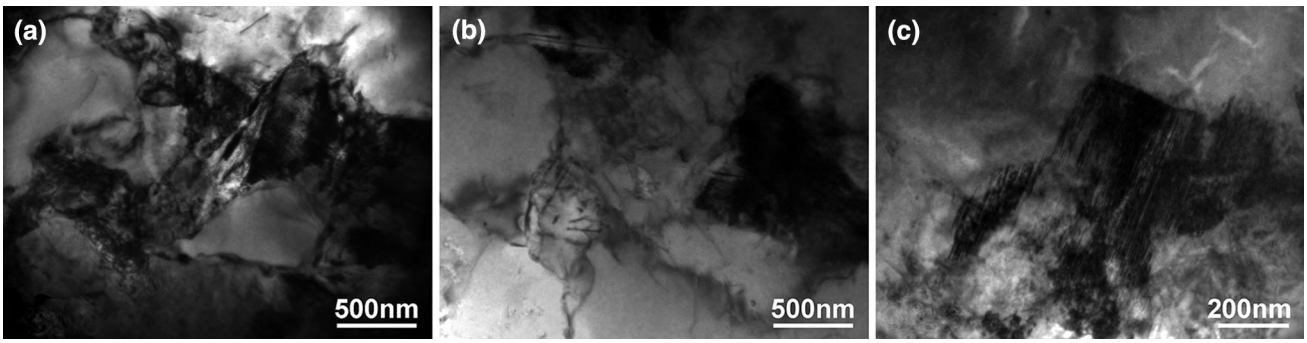

Fig. 5 TEM micrographs showing the microstructures of specimens No. 1 **a**, No. 2 **b**, No. 3 **c**

martensite. Higher carbon content austenite remains to room temperature.

Due to the difference in microstructures, the three specimens have different mechanical properties. When annealing at low temperature, there are some pearlite colonies and carbides which pin the dislocations. Therefore, YS is high, and yield point elongation is obvious. When annealing temperature is relatively high, the volume fraction of pearlite is decreased and a large amount of martensite is formed. Effected by martensite transformation, mobile dislocations are generated in ferrite grains. So YS is decreased, and yield point elongation becomes small. When annealing temperature is increased to 850 °C, there is no pearlite in microstructure, and martensite volume percentage reaches 19.6%. A mass of mobile dislocations is generated in ferrite grains, which is beneficial to eliminate yield point elongation [7]. Meanwhile, due to the increased volume fraction of martensite, tensile strength is increased.

In order to gain insight into the microstructures in relation to the deformation mechanisms, further TEM studies were conducted on deformation microstructure of specimen No. 1 and No. 3 after tensile test, as presented in Fig. 6. It is shown in Fig. 6a that a lot of dislocation tangles are distributed in the deformed ferrite matrix, while there are a lot of dislocation cells throughout the deformed ferrite matrix as shown in Fig. 6c. This indicated that movable dislocations in specimen No. 3 have more than specimen No. 1, so there is yield point elongation for specimen No. 1, while the yield elongation is disappeared in specimen No. 3. As shown in Fig. 6b, for specimen No. 1, it is readily to see that the martensite is extensively deformed and elongated in the tensile direction. Compared to the specimen No. 3, the deformed substructure in ferrite is less well developed. However, strain localization and substructure formation in specimen No. 3 are intense in ferrite, particularly close to ferrite/martensite interfaces. Martensite cracking and

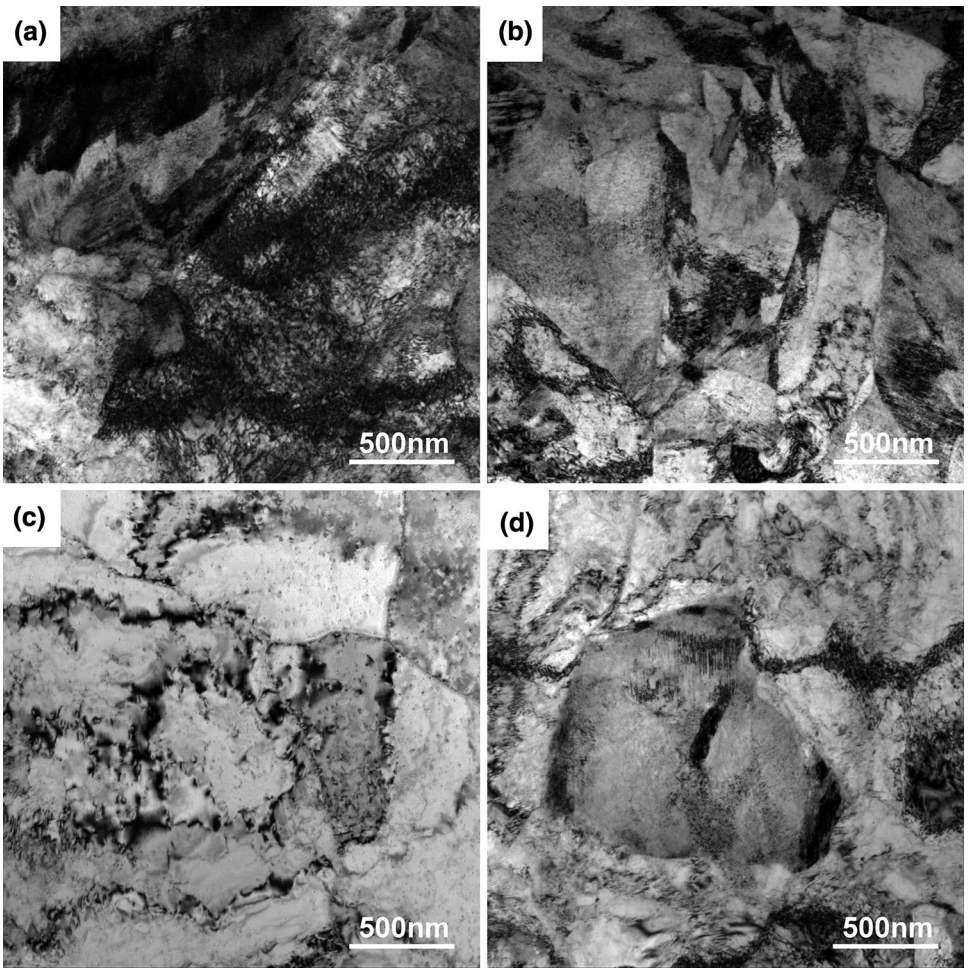

Fig. 6 TEM micrographs showing the deformed microstructures of specimens No. 1 **a**, **b** ; No. 3 **c**, **d**

interface decohesion are commonplace, while plastic deformation of martensite is not obvious.

4 Conclusions

Effect of the heat treatment parameters on microstructural characterization and strength–ductility balance has been investigated for hot-dip galvanizing DP780 steel. The deformation and fracture mechanism have also been discussed based on tensile test data and microstructure observations. The following conclusions can be drawn out:

(1) The YS of DP steel is sensitive to annealing schedule, while TEL has no noticeable dependence on annealing schedule.
(2) Sufficient movable dislocations within ferrite grains and high martensite volume fraction can eliminate yield point elongation, decrease the YS, and increase UTS.
(3) Increasing annealing temperature promotes austenite transformation into twin martensite, and increases volume fraction of martensite at sufficient cooling rate. With increasing the martensite volume fraction, the deformation substructure in the ferrite is well developed.

Acknowledgments This work was financially supported by the National Basic Research Program of China (No. 2011CB606306-2) and Fundamental Research Funds for the Central Universities (No. N110607005). The authors are very grateful to the reviewer for constructive and valuable comments.

References

[1] A. Kamp, S. Celotto, D.N. Hanlon, Mater. Sci. Eng. A **538**, 35 (2012)
[2] L. Chen, Y. Zhao, X. Qin, Acta Metall. Sin. (Engl. Lett.) **26**, 1 (2013)
[3] H. Huh, S. Kim, J. Song, J. Lim, Int. J. Mech. Sci. **50**, 918 (2008)

[4] X. Sun, K.S. Choi, A. Soulami, W.N. Liu, M.A. Khaleel, Mater. Sci. Eng. A **526**, 140 (2009)
[5] P. Tsipouridis, E. Werner, C. Krempaszky, E. Tragl, Steel Res. Int. **77**, 654 (2006)
[6] G. Gruben, E. Fagerholt, O.S. Hopperstad, T. Borvik, Eur. J. Mech. A Solid **30**, 204 (2011)
[7] M.S. Rashid, Annu. Rev. Mater. Sci. **11**, 245 (1981)
[8] Y. Granbom, Steel Res. **79**, 297 (2008)
[9] P. Movahed, S. Kolahgar, S.P.H. Marashi, M. Pouranvari, N. Parvin, Mater. Sci. Eng. A **518**, 1 (2009)
[10] R.R. Mohanty, O.A. Girina, N.M. Fonstein, Metall. Mater. Trans. A **42**, 3680 (2011)
[11] H. Liu, F. Li, W. Shi, S. Swaminathan, Y. He, M. Rohwerder, L. Li, Surf. Coat. Technol. **206**, 3428 (2012)
[12] S. Alibeigi, R. Kavitha, R.J. Meguerian, J.R. McDermid, Acta Mater. **59**, 3537 (2011)
[13] R. Khondker, A. Mertens, J.R. McDermid, Mater. Sci. Eng. A **463**, 157 (2007)
[14] M. Sarwar, R. Priestner, J. Mater. Sci. **31**, 2091 (1996)
[15] M. Erdogan, J. Mater. Sci. **37**, 3623 (2002)
[16] M. Radu, J. Valy, A. Gourgues, F.L. Strat, A. Pineau, Scr. Mater. **52**, 525 (2005)
[17] T. Sakaki, K. Ohnuma, K. Sugimoto, Y. Ohtakara, Int. J. Plast **6**, 591 (1990)
[18] Z. Jiang, Z. Guan, J. Lian, Mater. Sci. Eng. A **190**, 55 (1995)
[19] G. Rosenberg, I. Sinaiová, L. Juhar, Mater. Sci. Eng. A **582**, 347 (2013)
[20] M. Sarwar, T. Manzoor, E. Ahmad, N. Hussain, Mater. Des. **28**, 1928 (2007)
[21] J. Kadkhodapour, S. Schmauder, D. Raabe, S. Ziaei-Rad, U. Weber, M. Calcagnotto, Acta Mater. **59**, 4387 (2011)
[22] M.H. Saleh, R. Priestner, J. Mater. Process. Technol. **113**, 587 (2001)
[23] M. Calcagnotto, Y. Adachi, D. Ponge, D. Raabe, Acta Mater. **59**, 658 (2011)
[24] G.R. Speich, in *Fundamentals of Dual Phase Steels*, ed. by R.A. Kot, B.L. Bramfitt (AIME, New York, 1981), pp. 3–45
[25] P.K. Ray, R.I. Ganguly, A.K. Panda, Steel Res. **73**, 347 (2002)
[26] S. Tekeli, A. Güral, Mater. Sci. Eng. A **406**, 172 (2005)